2020

Model predictive control of layer width in wire arc additive manufacturing

Chunyang Xia
University of Wollongong, cx772@uowmail.edu.au

Zengxi Stephen Pan
University of Wollongong, zengxi@uow.edu.au

Shiyu Zhang
University of Wollongong, sz946@uowmail.edu.au

Joseph W. Polden
University of Wollongong, jpolden@uow.edu.au

Long Wang
University of Wollongong, lw010@uowmail.edu.au

See next page for additional authors

Model predictive control of layer width in wire arc additive manufacturing

Abstract

© 2020 The Society of Manufacturing Engineers Wire arc additive manufacturing (WAAM) is an emerging technology in the manufacturing industry, which uses a welding arc as an energy source to fuse metal wire and deposit layer by layer. In order to promote its manufacture precision, stability, and repeatability, it's crucial to develop a feedback control strategy for WAAM. This research implements vision-based feedback control for the layer width during the WAAM process. A WAAM system is developed using a robot and CMT welder with a visual sensing system. The dynamics of the layer width in WAAM process is modeled experimentally. An ARX dynamic model is built. Based on this model, a model predictive control (MPC) strategy is derived to regulate the WAAM process. Feedback control experiments were conducted to verify the tracking and robustness performance of the proposed MPC algorithm.

Disciplines

Engineering | Science and Technology Studies

Publication Details

Xia, C., Pan, Z., Zhang, S., Polden, J., Wang, L., Li, H., Xu, Y. & Chen, S. (2020). Model predictive control of layer width in wire arc additive manufacturing. Journal of Manufacturing Processes, 58 179-186.

Authors

Chunyang Xia, Zengxi Stephen Pan, Shiyu Zhang, Joseph W. Polden, Long Wang, Hui Jun Li, Yanling Xu, and Shanben Chen

Model predictive control of layer width in wire arc additive manufacturing

Chunyang Xia[a,b], Zengxi Pan[a,*], Shiyu Zhang[a], Joseph Polden[a], Long Wang[a], Huijun Li[a], Yanling Xu[b,*], Shanben Chen[b]

[a] School of Mechanical, Materials, Mechatronic and Biomedical Engineering, University of Wollongong, Wollongong, NSW, 2522, Australia

[b] School of Materials Science and Engineering, Shanghai Jiao Tong University, Shanghai 200240, China

Abstract: Wire arc additive manufacturing (WAAM) is an emerging technology in the manufacturing industry, which uses a welding arc as an energy source to fuse metal wire and deposit layer by layer. In order to promote its manufacture precision, stability, and repeatability, it's crucial to develop a feedback control strategy for WAAM. This research implements vision-based feedback control for the layer width during the WAAM process. A WAAM system is developed using a robot and CMT welder with a visual sensing system. The dynamics of the layer width in WAAM process is modeled experimentally. An ARX dynamic model is built. Based on this model, a model predictive control (MPC) strategy is derived to regulate the WAAM process. Feedback control experiments were conducted to verify the tracking and robustness performance of the proposed MPC algorithm.

Keywords: Additive Manufacturing; Vision; WAAM; MPC; Feedback control.

1. Introduction

Additive manufacturing (AM), also named as 3D printing or Directed Energy Deposition, has made revolutionary changes to the modern manufacturing industry. In comparison to traditional subtractive manufacturing, additive manufacturing fabricates components layer by layer through adding material, in forms of powder or wire. Thus additive manufacturing technology has extensive application prospects in repairing and direct shaping due to its limitless freedom in design [1]. Metal AM could be categorized according to its feedstock type (powder bed, powder-feeding and wire-feeding) or heat source form [2] (laser beam, welding arc and electron beam). Wire arc additive manufacturing (WAAM) utilizes welding arc as the energy of fusion to melt metal wire, which has attracted booming research interest during recent years [3]. Although the concept of

WAAM emerged in recent years, depositing the entire component using weld metal has been in practice since 1925 [4]. Compared to other AM technologies, WAAM advantages in aspects of high deposition rate. The deposition rate of WAAM is able to achieve 50–130 g/min, while the deposition efficiency for laser-based processes is to 2–10 g/min. This advantage makes WAAM highly suitable for fabricating large scale metal components [5, 6]. At the same time, it has the advantages of low equipment cost, environmental friendliness and great mechanical properties [3]. Due to those advantages, WAAM has wide prospects of application in various industries, including aerospace [7], shipbuilding [8] and architecture [9].

Recently, an increasing number of researches have been concentrating on WAAM, especially in aspects of path planning, microstructure evolution and process simulation. For example, Ding et al. developed an algorithm to plan optimal tool-paths for WAAM automatically [10]. Abe et al [11] used nickel-based alloy and stainless steel to achieve dissimilar metal deposition for WAAM. Zhou et al. [12] simulated the arc and metal transport in WAAM. However, the research effort on monitoring and control for WAAM is still insufficient. During the WAAM deposition process, various bead geometry may be required, especially for the complex component. Besides, the tool path of WAAM is set before deposition, which demands the bead geometry controllable. Otherwise, the depositing accuracy and surface planeness can't be guaranteed. One way to control the bead geometry is to establish a geometry prediction model offline. For example, Xiong et al [13] proposed to use a neural network model to predict the bead width and height for WAAM. Chen et al. proposed to utilize the XGBoost algorithm to model the correlation between process parameters and the height of the MAG welding bead. However, those offline predictive model can’t deal with the time-varying system and external disturbance. Especially when WAAM is deposited by multiple layers and multiple paths, the heat accumulation phenomenon is serious, thus the predictive model will inevitably mismatch. Besides, the disturbance may appear during the WAAM process, such as the shift of machine and environment disturbance. Therefore, a real-time feedback control strategy needs to be developed for WAAM.

At present, the research effort on additive manufacturing process control mainly concentrates on laser-based AM fields [14-17]. In current studies, feedback control strategies for layer geometry in WAAM are still insufficient. Only several researchers proposed the corresponding control method for the WAAM process. Such as Doumanidis et al [18] developed a multi-variable adaptive controller for the WAAM process, which is based on generalized one step ahead control algorithm. Xiong [19] et al proposed to use a single neuron self-learning controller

to regulate the bead width during WAAM. Besides, a model-identification adaptive controller (MIAC) was developed by Xiong [20] to control the bead height during the WAAM process.

Model predictive control (MPC) has attracted extensive interest during recent decades due to its robustness to model uncertainty and capability of dealing with system constraints. Therefore MPC is suitable for AM process control. In welding fields, MPC has been applied to control the welding penetration [21-25]and melt pool morphology [26]. However, in the additive manufacturing field, there is still no report that the MPC algorithm has been used to control the depositing geometry. One of the main goals of this study is to introduce MPC to the reader and illustrate its potential application in the field of metal additive manufacturing.

This paper is organized as follows. In section 2, the experimental equipment is introduced, and the vision-based sensing system is presented. In section 3, an experiment of system identification is designed, and the liner ARX model is utilized to model the relationship between wire feed speed and bead width. Then, the MPC algorithm is derived in section 4, and simulation is implemented. In order to further test the tracking performance and robustness, experiments are implemented and discuss in section 5. Section 6 concludes this paper.

2. Experiment system

The wire arc additive manufacturing system is shown in Figure 1, which consisted of an ABB robot, a Fronius CMT welder, a vision-based sensing system, and a computer used for controlling. The shielding gas consisted of 80% Ar and 20% CO_2. The wire is 0.9 mm diameter of mild steel. The robot control cabinet is used for coordinating robot movements and welding processes. The real-time adjustment of WFS (wire feed speed) is implemented by changing the analogy input of the welder. The welding current and voltage were matched automatically by Fronius CMT welder according to the WFS.

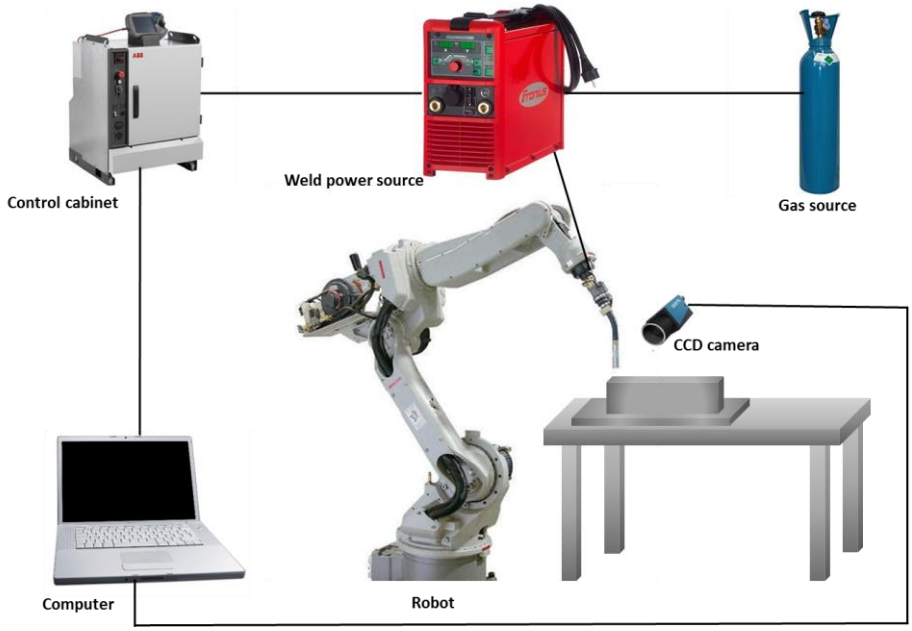

Figure 1 Schematic diagram of the WAAM system

A passive visual sensor, which consisted of a CCD camera, 650 nm narrow-band filter and dimmers was used to capture the bead images. This aims to restrain the strong arc and infra-red radiation from high-temperature liquid metal. The high-temperature melt pool is in liquid form under the electric arc. Thus the deposited layer geometrical dimension is still uncertain. Therefore, the CCD camera was fixed at the backside of the welding gun, and the width of the tailing part of the melt pool can be measured.

In order to reduce the computation and save CPU time, ROI (region of interest) was extracted. During the WAAM process, the noise from arc light and electromagnetic interference may deteriorate the quality of the image. Therefore an adaptive wiener filter algorithm was used to restrain those noise. Then the edge of the welding pool can be extracted, and width can be calculated. In this study, a Canny Edge Detector was utilized to detect the edge. The flowchart of image processing is illustrated in Figure 2. A simple calibration of the camera was implemented. The relationship between the dimension in an image and the real world in the width direction is obtained. The actual width of a single pixel in the bead width direction is 0.03 mm/pixel. Therefore the actual width of the melt pool can be calculated as the following equation.

$$Width_{actual} = 0.03 Width_{img} \quad (1)$$

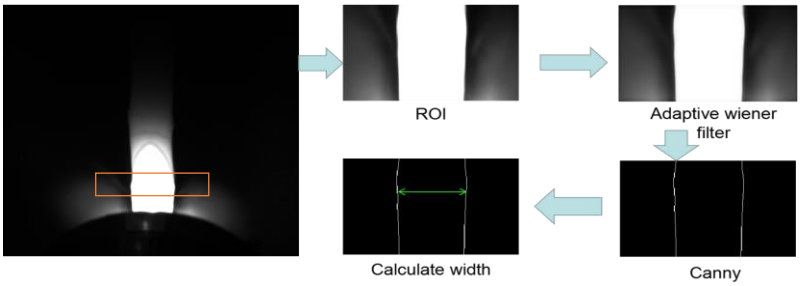

Figure 2 Flow chart of image processing

3. System identification

Normally, controllers are designed according to the dynamic characteristics of the system. During the WAAM process, the WFS (wire feed speed) has the most obvious effect on bead width. In this study, the WFS (wire feed speed) was chosen as the system input, and system output was the bead width. In order to design an ideal controller, the dynamic model, which describes the dynamic relationship between system input and output, needs to be established.

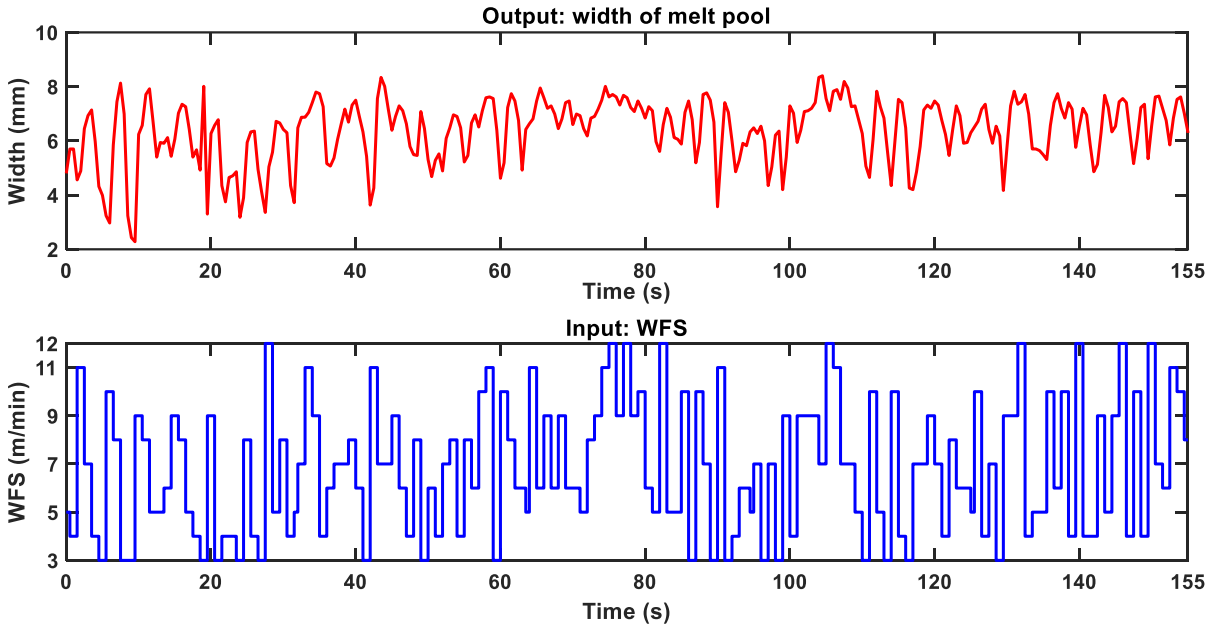

Figure 3 system identification

Dynamic experiments were conducted. In order to achieve that input data continuously stimulating the dynamic process, the WFS was designed to change randomly. The system input of WFS varied randomly between 3-12 m/min, as shown in Figure 3, and the corresponding melt pool width could be obtained. According to previous related literature[19, 27], the sampling period in this paper was set at 0.5s. Other experiment parameters are listed in Table 1.

Parameters	Value
Welding speed	5 mm/s
Ar (80%) and CO_2 (20%) gas flow	25
Wire electrode diameter	0.9mm
Size of mild steel substrate	300×150×10

Table 1 experimental condition of WAAM

In most cases, the nonlinear model can be linearized to a linear discrete model. It is well known that MPC strategies possess instinctive robustness properties, so that accurate control can be achieved even though the main dynamic of a system is approximated with low-order linear models. In this study, the controlled process was modeled in the linear ARX form. ARX model can be expressed as:

$$A(z)y(k) = B(z)u(k) + e(k) \tag{2}$$

A(z) and B(z) are polynomials, and can be written as:

$$A(z) = 1 + a_1 z^{-1} + a_2 z^{-2} + \cdots + a_{n_a} z^{-n_a} \tag{3}$$

$$B(z) = b_0 + b_1 z^{-1} + b_2 z^{-2} + \cdots + b_{n_b} z^{-n_b} \tag{4}$$

a(j), j=1,…, n_a	b(j), j=1,…, n_b
[-0.493, -0.000041, 0.162, -0.092, -0.02, -0.046, -0.068, -0.02, -0.104]	[0.166, 0.123]

Table 2 Model parameters

Where y (k) is bead width, and u (k) is WFS, z^{-1} represents the delay operator, n_a and n_b are structural parameters, $e(k)$ is the noise. The system identification was implemented in MATLAB System Identification Toolbox. Figure 4 presents the prediction result for an independent testing dataset. The parameters of the identified dynamic model are listed in Table 2. The root means square error (RMSE) of the ARX model for testing dataset is 0.474, which is calculated as (5). It suggests that the layer width can be predicted by the model with acceptable accuracy.

$$RMSE = \sqrt{\frac{\sum_{K=1}^{N}(\hat{w}(k) - w(k))^2}{N}} \tag{5}$$

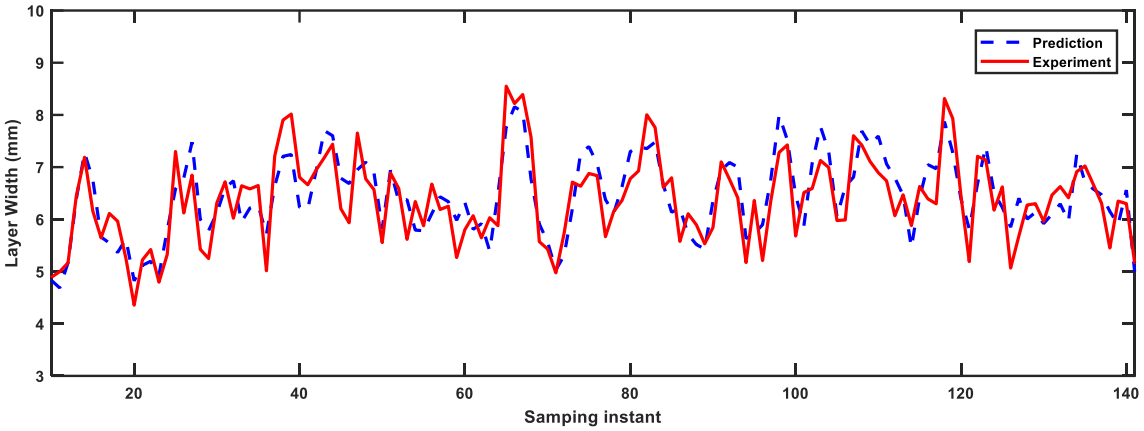

Figure 4 Validation of ARX model

4. MPC design

Model predictive control (MPC) has been considered as one of the most effective control algorithms, which has gained wide industrial applications. Just as its name indicates, MPC employs a dynamic model to estimate the future output of a system. A cost function could be obtained from the predictive output and desired output. Through optimizing the cost function, a set of input sequences could be computed, but only the first control input is implemented to the controlled system, according to the receding optimization strategy. The principle of MPC for WAAM is illustrated in Figure 5.

MPC algorithm owns robustness properties naturally, therefore the main dynamics of a system can be approximated with linear models. In this section, based on the ARX model, the model predictive control strategy for WAAM bead width is derived.

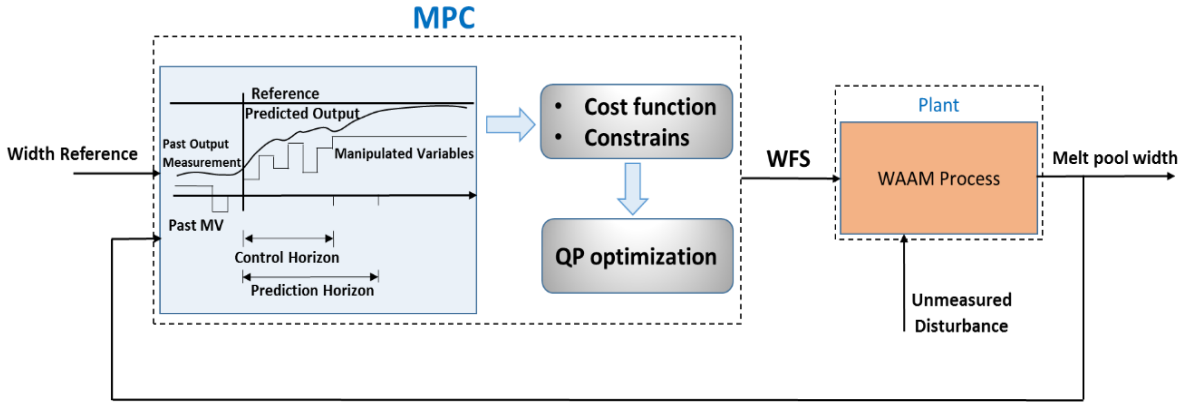

Figure 5 principle of MPC for WAAM

The ARX model (2) can be extended to n_j steps and written as:

$$y(k+1)+\sum_{i=1}^{n} a_i y(k+1-i)=\sum_{i=1}^{m} b_i u(k+1-i)$$
$$y(k+2)+\sum_{i=1}^{n} a_i y(k+2-i)=\sum_{i=1}^{m} b_i u(k+2-i)$$
$$\vdots$$
$$y(k+n_j)+\sum_{i=1}^{n} a_i y(k+n_j-i)=\sum_{i=1}^{m} b_i u(k+n_j-i) \tag{6}$$

Separating the future input and output variables after instant K from past input and output (before instant K), and (6) can be written in the matrix form:

$$\underbrace{\begin{bmatrix} 1 & 0 & \cdots & 0 \\ a_1 & 1 & \cdots & 0 \\ a_2 & a_1 & \cdots & 0 \\ \vdots & \vdots & \vdots & \vdots \end{bmatrix}}_{C_a} \underbrace{\begin{bmatrix} y_{k+1} \\ y_{k+2} \\ \vdots \\ y_{k+np} \end{bmatrix}}_{\vec{y}_{k+1}} + \underbrace{\begin{bmatrix} a_1 & a_2 & \cdots & a_{np+1} \\ a_2 & a_3 & \cdots & 0 \\ a_3 & a_4 & \cdots & 0 \\ \vdots & \vdots & \vdots & \vdots \end{bmatrix}}_{H_a} \underbrace{\begin{bmatrix} y_k \\ y_{k-1} \\ \vdots \\ y_{k-np+1} \end{bmatrix}}_{\overleftarrow{y}_k}$$
$$= \underbrace{\begin{bmatrix} b_1 & 0 & \cdots & 0 \\ b_2 & b_1 & \cdots & 0 \\ b_3 & b_2 & \cdots & 0 \\ \vdots & \vdots & \vdots & \vdots \end{bmatrix}}_{C_b} \underbrace{\begin{bmatrix} u_k \\ u_{k+1} \\ \vdots \\ u_{k+np-1} \end{bmatrix}}_{\vec{u}_k} + \underbrace{\begin{bmatrix} b_2 & b_3 & \cdots & b_{np} \\ b_3 & b_4 & \cdots & 0 \\ b_4 & b_5 & \cdots & 0 \\ \vdots & \vdots & \vdots & \vdots \end{bmatrix}}_{H_b} \underbrace{\begin{bmatrix} u_{k-1} \\ u_{k-2} \\ \vdots \\ u_{k-np+1} \end{bmatrix}}_{\overleftarrow{u}_{k-1}} \tag{7}$$

Expressing (7) in simple form:

$$C_a\vec{y}_{k+1}+H_a\overleftarrow{y}_k=C_b\vec{u}_k+H_b\overleftarrow{u}_{k-1} \tag{8}$$

Thus the future output $\vec{y}_{k+1}$ can be expressed as:

$$\vec{y}_{k+1}=(C_a)^{-1}(C_b\vec{u}_k+H_b\overleftarrow{u}_{k-1}-H_a\overleftarrow{y}_k) \tag{9}$$

The implementation of an MPC typically needs to minimize a cost function [28]. The cost function is selected as (10):

$$J=\lambda_Q\left\|\vec{R}-\vec{y}_{k+1}\right\|^2+\lambda_p\left\|\Delta\vec{u}\right\|^2 \tag{10}$$

The first term in cost function penalizes the deviations between predicted output $\vec{y}_{k+1}$ and reference trajectory $\vec{R}$. And the second term is used to penalize the change rate of input. λ_Q and λ_p are positive-definite weight factors, which represent the relative contributions of these two terms, and influence the outcome of optimization. When λ_p increases, $\Delta u[k]$ will decrease. In this study, $\lambda_Q=1$, $\lambda_p=0.1$.

If the liner model is not expressed in incremental form, $\Delta\vec{u}$ can be express as (11):

$$\Delta\vec{u} = \begin{bmatrix} u(k) - u(k-1) \\ \vdots \\ u(k+n_c-1) - u(k+n_c-2) \\ \vdots \end{bmatrix}$$

$$= \begin{bmatrix} 1 & 0 & 0 & \cdots & 0 \\ -1 & 1 & 0 & \cdots & 0 \\ 0 & -1 & 1 & \cdots & 0 \\ \vdots & \vdots & \vdots & \vdots & \vdots \\ 0 & 0 & \cdots & -1 & 1 \end{bmatrix} \vec{u}_k - \begin{bmatrix} 1 & 0 & 0 & \cdots & 0 \\ 0 & 0 & 0 & \cdots & 0 \\ 0 & 0 & 0 & \cdots & 0 \\ \vdots & \vdots & \vdots & \vdots & \vdots \\ 0 & 0 & \cdots & 0 & 0 \end{bmatrix} \overleftarrow{u}_k$$

$$= C_f\vec{u}_k - C_p\overleftarrow{u}_{k-1} \quad (11)$$

n_c is the control horizon, n_j is the predictive horizon. The control horizon is the number of steps after that the control input will be constant when estimating the future output of the system. Substitute (9) and (11) into (10), the cost function can be expressed in:

$$J = \lambda_Q \left\| \vec{R} - \left(C_a\right)^{-1}(C_b\vec{u}_k + H_b\overleftarrow{u}_{k-1} - H_a\overleftarrow{y}_k) \right\|^2 + \lambda_p \left\| C_f\vec{u}_k - C_p\overleftarrow{u}_{k-1} \right\|^2 \quad (12)$$

The optimization of the cost function is constrained, because of the allowable ranges of both outputs and input variables. In this study, the input is constrained by the limitation of the welding machine. The control input WFS is constrained as:

$$\vec{u}_{min} \le \vec{u}_k \le \vec{u}_{max} \quad (13)$$

Therefore, the solution of $\vec{u}_k$ is a quadratic programming problem (QP) [29]. Writing the cost function and constrain in QP form:

Minimize:

$$\frac{1}{2}\vec{u}_k^T H\vec{u}_k + F\vec{u}_k$$

Subject to:

$$A\vec{u}_k \le b \quad (14)$$

In above,

$H = 2\lambda_Q C_a^{-1}(C_a^{-1})^T C_b C_b^T + \lambda_P C_f C_f^T$

$F = 2\lambda_Q C_a^{-1}(C_a^{-1})^T C_b(H_b\overleftarrow{u}_{k-1} - H_a\overleftarrow{y}_k) - 2\lambda_p C_f C_p\overleftarrow{u}_{k-1} - 2(\lambda_Q\vec{\mathrm{R}}C_a^{-1}C_b)^T$

$\mathrm{A} = \begin{bmatrix} I \\ -I \end{bmatrix}, b = \begin{bmatrix} u_{max} \\ -u_{min} \end{bmatrix},$

At present, Many QP solvers are available, such as CVX [30], MTP[31] and YALMIP[32]. In this study, the control program was developed in C# language to communicate with different equipment (sensors, robot and welding machine) and implement real-time computation. A C# mathematics library (CenterSpace.NMath [33]) was applied to solve the QP optimization problem real-time. CenterSpace.NMath library is a convenient commercial mathematical class library, which is fast in running and easy for implementation. After testing, it's found that the computing time for solving QP problem in our C# program is 120-150 ms.

At every step, H and F will be updated, and then optimization can be implemented to calculate control input WFS. The whole MPC algorithm for WAAM bead width control is illustrated in Figure 6. When getting the optimal control input sequence through solving the QP problem, only the first item of the input array is actually implemented to the plant, and the rest of the optimal input is neglected. At the next time instant, the procedure of the proposed algorithm is repeated; A newly measured y_k is applied as an initial condition, with the cost function (12) moved one step ahead according to the receding horizon principle [21].

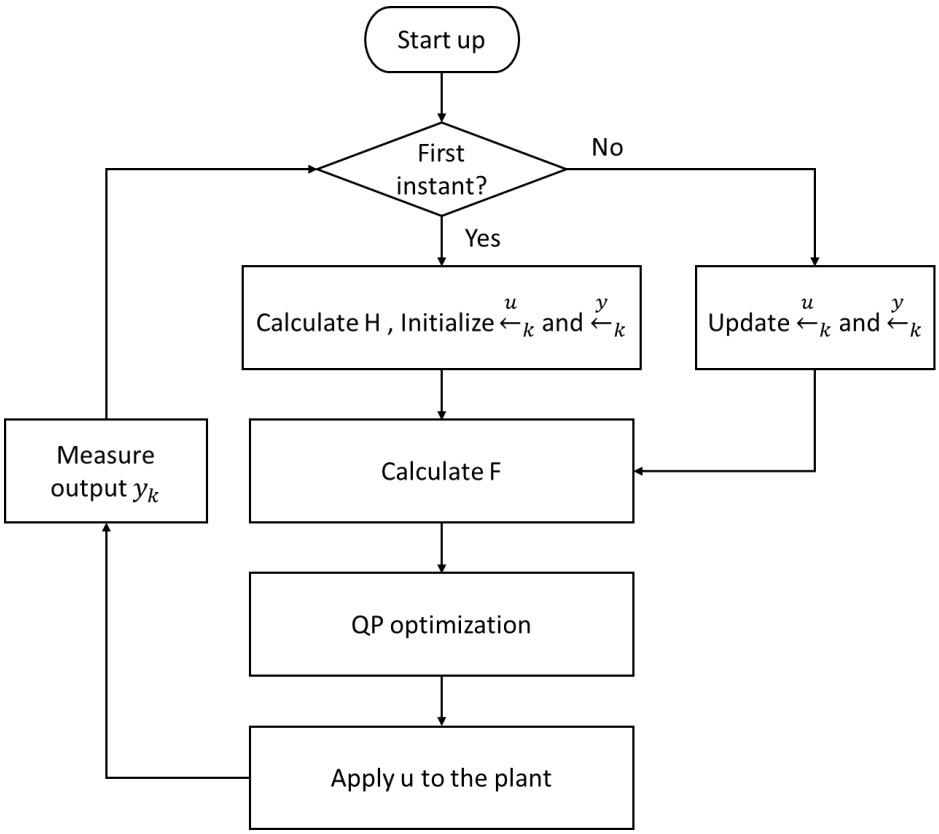

Figure 6 Algorithm flowchart of MPC in WAAM

4.1 Controller simulation

In order to validate the effectiveness of MPC for WAAM bead geometry control, a simulation was implemented and compared with the traditional PID controller. The performance of the PID controller relies on the tuning of controller parameters. In this paper, the PID tuner toolbox in MATLAB was used to optimize the parameters of the PID controller. The result shows that when the parameters of the PID controller are optimized as $K_p = 1.5$, $K_i = 0.2$, $K_d = -0.15$, the best tracking performance can be achieved.

As illustrated in Figure 7, the simulations of tracking varying set point and resisting disturbance were performed. Comparing the performance of the developed MPC controller with the traditional PID controller, it can be found that the MPC controller has an obvious smaller overshoot than PID, while the settling time of MPC and PID are almost the same. In order to evaluate the effectiveness and robustness of the proposed MPC controller furtherly, the tracking and robust testing experiments will be implemented in the next Section.

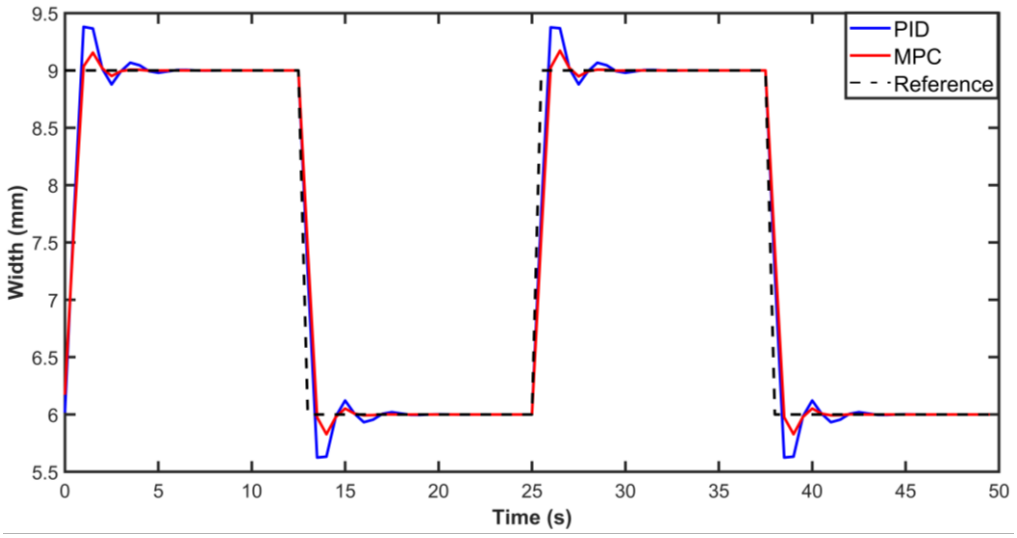

(a)

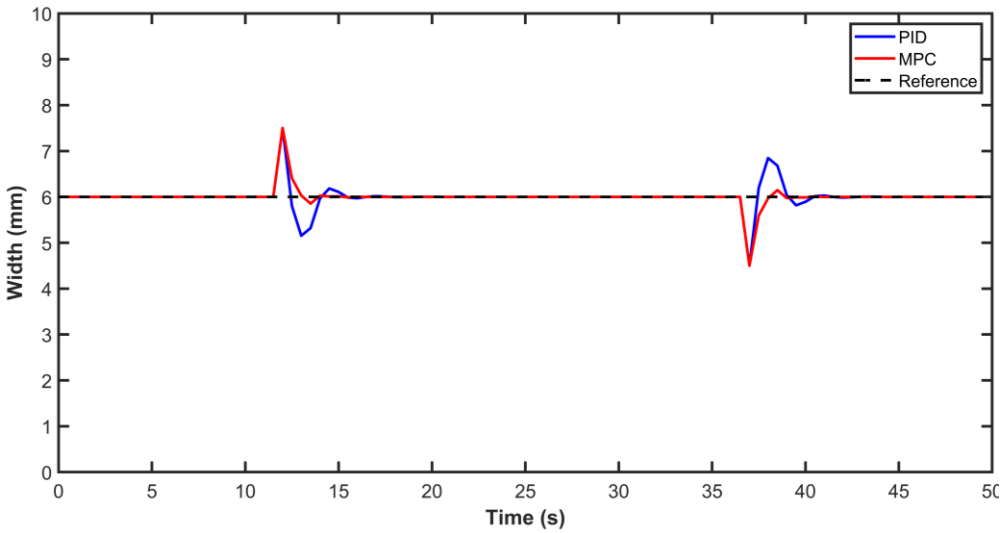

(b)

Figure 7 Simulation results (a) tracking varying set point (b) Disturbance resistance

5. Experiment results

To further validate the tracking performance and robustness of the proposed MPC algorithm for layer width control in WAAM, closed-loop control experiments are implemented. Welding beads were deposited on a substrate, which is a steel plate of 300×150×10. Er70s6 mild steel wire was utilized as the weld consume material. Ar (80%) and CO_2 (20%) shielding gas were utilized for protecting at a flow rate of 20 L/min. Besides, the welding speed was fixed at 5 mm/s.

First of all, the performance of the MPC controller for tracking various desired values is verified by the experiment. As shown in Figure 8, the reference point is set to increase from 6mm to 9 mm. It can be seen that the MPC is able to track a higher set-value with little overshoot and acceptable speed. Besides, the MPC controller is able to track a lower reference point. As illustrated in Figure 9, when the reference point decrease from 8.5 mm to 5.5 mm, the controller is capable of tuning the WFS according to bead width feedback, and the bead width could be controlled at desired set-points. From the above experiments, it can be seen that this proposed MPC algorithm is capable of controlling the process with good effect.

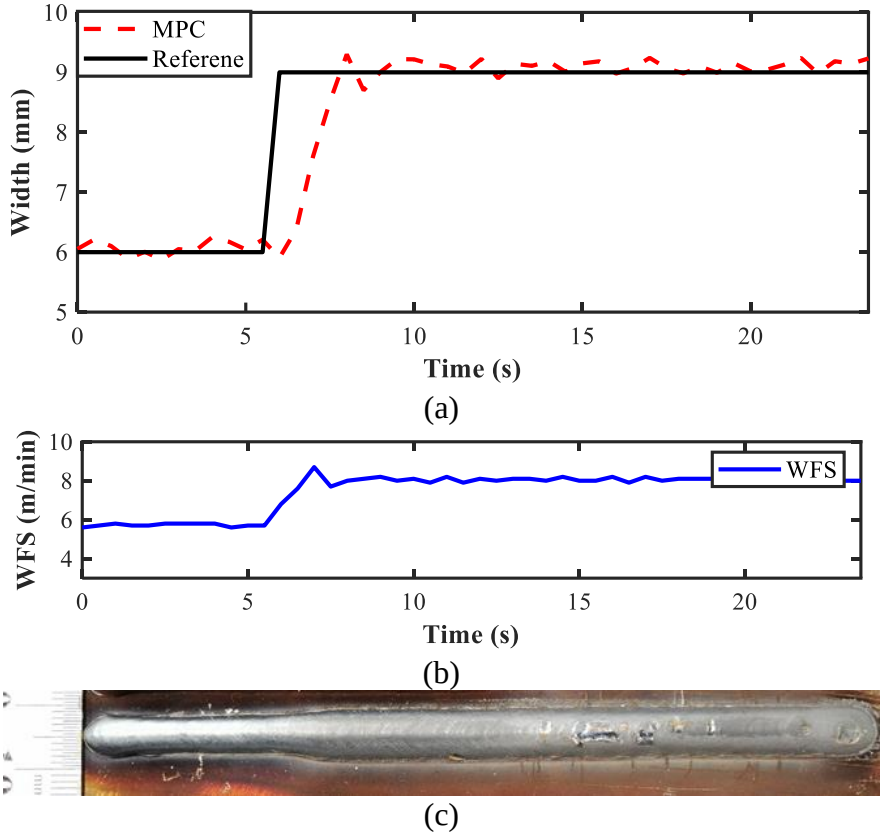

Figure 8 Performance of tracking increasing set-point

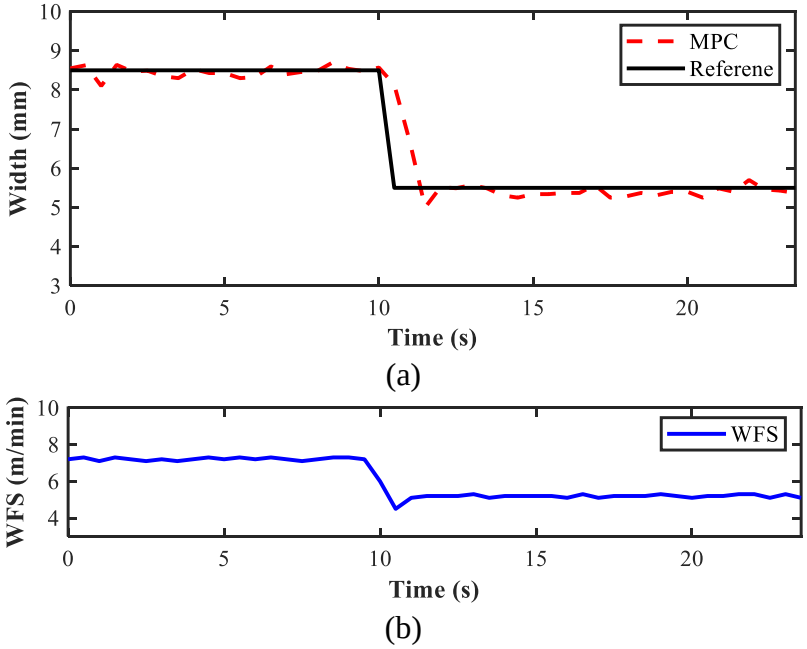

(c)

Figure 9 Performance of tracking decreasing set-point

Furthermore, the robustness of this MPC controller is evaluated by introducing the WFS disturbance. During the WAAM process, the WFS was switched to a higher value at t=7s, and then the bead width began to decrease. At the next sampling instant, the change in width will be fed back to the controller, and then the MPC controller will adjust the WFS to make the width return to the desired set-point. The system input and output under WFS disturbance are illustrated in Figure 10. It can be observed that the controller was capable to deal with the disturbance and maintain the layer width to the desired value. It took 3 sampling intervals to implement the resistance of disturbance with a small overshoot. Due to the intrinsic delay nature of metal melting and flowing process in WAAM, it took a relatively long time to achieve steady-state response to the change of input signal. Also, due to the strong disturbance, the overshoot was generated during the adjusting process, and it need to take one sampling interval to eliminate the deviation of overshoot. Therefore, 3 sampling intervals were needed to achieve the rejection of the disturbance. This experiment was designed under a special case to verify the robustness of the proposed controller. In practical application, there is little chance to generate such a strong disturbance. Therefore the controller's robustness performance is acceptable in WAAM application.

Figure 11 presents a width-varying wall, which is deposited under the control of the proposed MPC controller. Figure 12 presents the layer width and used WFS in the 1th layer, 2th layer, 6th layer and 8th layer during deposition. It can be seen that the layer width can be controlled well in each layer. With the increase of deposited layers, the WFS used to maintain the same layer width has a slight declining trend. This can be explained by the change of thermal boundary for different layers during the deposition process.

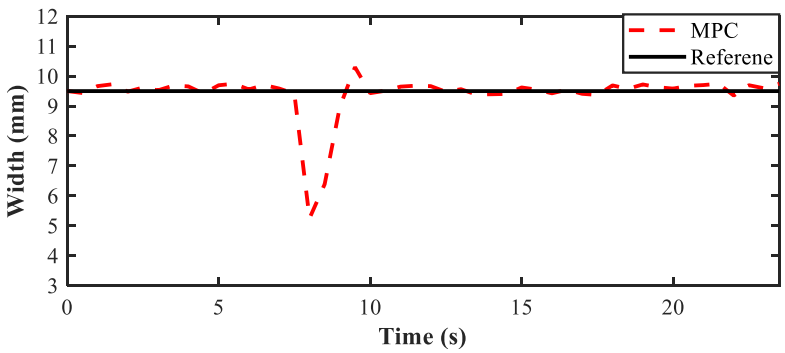

(a)

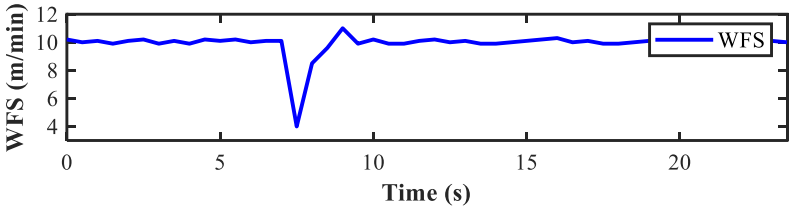

(b)

(c)

Figure 10 Performance of disturbance resistance

Figure 11 Width-varying wall

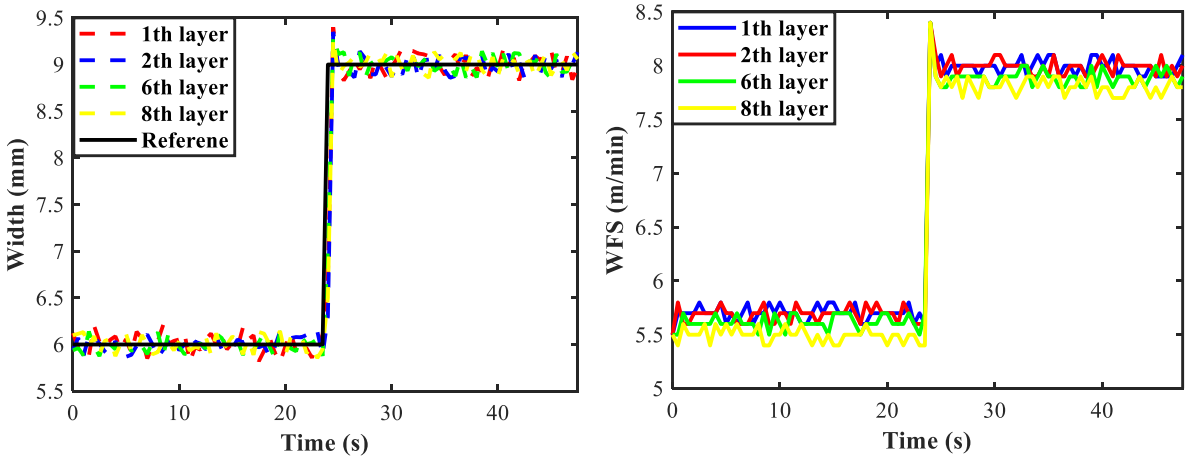

(a) (b)

Figure 12 Control output and input (a). Layer width (b). WFS

6. Conclusion

This study aims to apply the MPC algorithm to control the layer width during the WAAM process. The welding pool images were captured by a passive visual sensor. Image processing algorithms, such as the adaptive wiener filter and the Canny algorithm, were utilized to obtain vital information. A linear ARX model was identified through the least-squares algorithm. An optimal MPC controller was designed to control the layer width. Simulation results show its effectiveness in tracking performance and robustness is better than the traditional PID controller. Various tracking experiments were implemented to further validate the proposed optimal MPC controller. The controller is capable of tracking the desired trajectory with acceptable accuracy. The feedback control experiments also verified the robustness of the MPC controller in resisting disturbance by introducing an abrupt change in WFS.

Acknowledgments

The authors gratefully acknowledge the China Scholarship Council for financial support (NO. 201704910782) and UOW Welding and Industrial Automation Research Centre.

Reference

1. Levy, G.N., R. Schindel, and J.-P. Kruth, *Rapid manufacturing and rapid tooling with layer manufacturing (LM) technologies, state of the art and future perspectives.* CIRP annals, 2003. **52**(2): p. 589-609.
2. Frazier, W.E., *Metal additive manufacturing: a review.* Journal of Materials Engineering and Performance, 2014. **23**(6): p. 1917-1928.
3. Cunningham, C.R., et al., *Invited review article: Strategies and processes for high quality wire arc additive manufacturing.* Additive Manufacturing, 2018. **22**: p. 672-686.
4. Ralph, B., *Method of making decorative articles*. 1925, Google Patents.
5. Bai, J., et al., *Effects of thermal cycles on microstructure evolution of 2219-Al during GTA-additive manufacturing.* The International Journal of Advanced Manufacturing Technology, 2016. **87**(9-12): p. 2615-2623.
6. Li, F., et al., *Evaluation and optimization of a hybrid manufacturing process combining wire arc additive manufacturing with milling for the fabrication of stiffened panels.* Applied Sciences, 2017. **7**(12): p. 1233.
7. *Stelia aerospace use WAAM build an airplane fuselage*. Available from: https://3dprintingindustry.com/news/stelia-aerospace-use-waam-build-airplane-fuselage-129192/.
8. *Naval group and centrale nantes use WAAM to 3D print the world's first hollow propeller blade*. Available from: https://3dprintingindustry.com/news/naval-group-and-centrale-nantes-use-waam-to-3d-print-the-worlds-first-hollow-propeller-blade-148700/.
9. *MX3D Bridge*. Available from: https://mx3d.com/projects/bridge-2/.
10. Ding, D., et al., *A tool-path generation strategy for wire and arc additive manufacturing.* The international journal of advanced manufacturing technology, 2014. **73**(1-4): p. 173-183.
11. Abe, T. and H. Sasahara, *Dissimilar metal deposition with a stainless steel and nickel-based alloy using wire and arc-based additive manufacturing.* Precision Engineering, 2016. **45**: p. 387-395.
12. Zhou, X., et al., *Three-dimensional numerical simulation of arc and metal transport in arc welding based additive manufacturing.* International Journal of Heat and Mass Transfer, 2016. **103**: p. 521-537.
13. Xiong, J., et al., *Bead geometry prediction for robotic GMAW-based rapid manufacturing through a neural network and a second-order regression analysis.* Journal of Intelligent Manufacturing, 2014. **25**(1): p. 157-163.
14. Hofman, J.T., et al., *A camera based feedback control strategy for the laser cladding process.* Journal of Materials Processing Technology, 2012. **212**(11): p. 2455-2462.
15. Iravani-Tabrizipour, M. and E. Toyserkani, *An image-based feature tracking algorithm for real-time measurement of clad height.* Machine Vision and Applications, 2007. **18**(6): p. 343-354.
16. Moralejo, S., et al., *A feedforward controller for tuning laser cladding melt pool geometry in real time.* The International Journal of Advanced Manufacturing Technology, 2016. **89**(1-4): p. 821-831.
17. Shi, T., et al., *Closed-loop control of variable width deposition in laser metal deposition.* The International Journal of Advanced Manufacturing Technology, 2018. **97**(9-12): p. 4167-4178.
18. Doumanidis, C. and Y.-M. Kwak, *Geometry modeling and control by infrared and laser sensing in thermal manufacturing with material deposition.* Journal of manufacturing science and engineering, 2001. **123**(1): p. 45-52.
19. Xiong, J., Z. Yin, and W. Zhang, *Closed-loop control of variable layer width for thin-walled parts in wire and arc additive manufacturing.* Journal of Materials Processing Technology, 2016. **233**: p. 100-106.
20. Xiong, J. and G. Zhang, *Adaptive control of deposited height in GMAW-based layer additive manufacturing.* Journal of Materials Processing Technology, 2014. **214**(4): p. 962-968.
21. Zhang, Y.M., R. Kovacevic, and L. Li, *Adaptive control of full penetration gas tungsten arc welding.* IEEE Transactions on Control Systems Technology, 1996. **4**(4): p. 394-403.
22. Zhang, Y.M. and R. Kovacevic, *Neurofuzzy model-based predictive control of weld fusion zone geometry.* IEEE Transactions on Fuzzy Systems, 1998. **6**(3): p. 389-401.
23. Yu Kang, L. and Z. Yu Ming, *Model-Based Predictive Control of Weld Penetration in Gas Tungsten Arc Welding.* IEEE Transactions on Control Systems Technology, 2014. **22**(3): p. 955-966.
24. Liu, Y.K. and Y.M. Zhang, *Model-based predictive control of weld penetration in gas tungsten arc welding.* IEEE Transactions on Control Systems Technology, 2013. **22**(3): p. 955-966.

25. Lu, Y., et al., *Predictive control based double-electrode submerged arc welding for filet joints.* Journal of Manufacturing Processes, 2014. **16**(4): p. 415-426.
26. Liu, Y. and Y. Zhang, *Control of 3D weld pool surface.* Control Engineering Practice, 2013. **21**(11): p. 1469-1480.
27. Liu, Y. and Y. Zhang. *Adaptive modeling of the weld pool geometry in gas tungsten arc welding*. in *2013 10th IEEE INTERNATIONAL CONFERENCE ON NETWORKING, SENSING AND CONTROL (ICNSC)*. 2013. IEEE.
28. Maciejowski, J.M., *Predictive control: with constraints*. 2002: Pearson education.
29. Garcia, C.E. and A. Morshedi, *Quadratic programming solution of dynamic matrix control (QDMC).* Chemical Engineering Communications, 1986. **46**(1-3): p. 73-87.
30. Grant, M., S. Boyd, and Y. Ye, *cvx users' guide.* online: http://www. stanford. edu/~ boyd/software. html, 2009.
31. Kvasnica, M., et al. *Multi-parametric toolbox (MPT)*. in *International Workshop on Hybrid Systems: Computation and Control*. 2004. Springer.
32. Löfberg, J. *YALMIP: A toolbox for modeling and optimization in MATLAB*. in *Proceedings of the CACSD Conference*. 2004. Taipei, Taiwan.
33. *CenterSpace.NMath*. Available from: https://www.centerspace.net/doc/NMath/user/nonlinear-programming-88363.htm.